LIP-STUDENTS-22-05

Building a QCD parton shower

Diogo Costa[1,a] and A. Carolina Ribeiro[2,b]

[1] *Instituto Superior Técnico, Lisboa, Portugal*
[2] *Faculdade de Ciências da Universidade de Lisboa, Lisboa, Portugal*

Project supervisors: Liliana Apolinário, André Cordeiro, Guilherme Milhano

October 17, 2022

Abstract.
The analysis of jets, whose substructure encodes information about the evolution of the parton shower, a cascade of quarks and gluons, is essential when trying to reconstruct collision events. The splitting probabilities regarding parton showers can be calculated using perturbative QCD, this way the shower evolution can be simulated using a toy Monte Carlo. In this work we developed a simple parton shower model, choosing the invariant mass as the ordering variable while also assuming the quark to propagate without recoiling effects. We exploited the model in different ways and compared it with another one where the quark is allowed to deflect after each emission. Regarding the first model, we found an increase in the gluon energy fraction z and a decrease in the angle θ between the gluon and the quark as we go further in each emission. By increasing the initial momentum we found a decrease regarding θ while z is unchanged. Finally, we also compared this model with the one considering the possibility of quark deflection and by doing so we found the same overall evolution as the first model, but with a trajectory along the phase space emissions much more pronounced.

Keywords: QCD, Sudakov form factors, parton shower

1 Introduction

In proton-proton (pp) and heavy-ion (AA) collisions, very energetic quarks and gluons are produced through hard scattering processes. As a consequence of being very energetic, they emit other partons (quarks and gluons) in a collimated cone. This collimated cascade of particles called a parton shower [1, 2], keeps developing until the energy of the partons reaches the order of the mesons' and baryons' rest mass. When this threshold is reached, hadronization takes place, and the newly formed hadrons propagate until they eventually reach the detectors. Despite the hadronization, the collimated signature of the parton shower is still measurable and we can group the final state particles into clusters, which we call jets [2, 3]. These structures can then be used to reconstruct the process backwards, starting from the list of final state particles to the hard-scattered ones.

The study of jets and their substructure in pp collisions lies in the direct connection of the parton showers to one of the building blocks of the Standard Model of Particle Physics: the Quantum Chromodynamics (QCD)[1, 2, 4]. Given its high energy scales, the description of parton showers can be made using first-principle perturbative methods. Moreover, these objects are also useful to investigate the properties of the new state of exotic matter that is produced in AA collisions (the Quark-Gluon Plasma - QGP), which behaves as an almost perfect liquid, and for which these jets are the main probes [5].

In this project, we will focus on pp collisions. For that, we developed a simple parton shower model that is based on the invariant mass - the particle rest mass, given by the Einstein energy relation in natural units ($c = \hbar = 1$) as $m^2 = E^2 - |\vec{p}|^2$ - as the ordering variable. In subsection 2.1 we start by explaining the initial conditions and assumptions underlying the model. We then present the algorithm details related to the variable boundaries in subsection 2.2 and actual generation using the Sudakov form factors in subsection 2.3. In subsection 2.4 we show how to compute the relevant kinematics, namely the angle θ between the emitted gluon and the daughter quark, and also the gluon energy fraction z with respect to its mother quark. Following that, in subsection 3.1 we show the evolution of the z and θ distributions as we go further in emissions. In subsection 3.2 we show the evolution of the z and θ distributions as we increase the initial momentum. In subsection 3.3 we finally show the comparison between both models (when considering or not the possibility for the quark to deflect as it emits gluons), regarding the differences in the z and θ distributions as we go further in emissions.

2 Parton Shower Algorithm

A parton shower algorithm is a sort of recipe to translate the initial hard-scattered parton (quark or gluon) into the collection of the final state partons before the hadronization stage [1, 2, 5, 6]. In essence, the algorithm dictates the types of processes that can occur, and in doing so it constrains the final state of particles and their distributions. In this way, the parton shower algorithm is responsible for the substructure of jets. Our model, for example, explains how one can go from a single energetic quark to a low energy quark and N gluons after N splittings.

When computing emission probabilities one often refers to the Sudakov form factors [2]. Particularly, in the considered conditions specified in subsection 2.1, we can compute the no emission probability between two scales

[a] e-mail: diogo.brito.da.costa@tecnico.ulisboa.pt
[b] e-mail: ana-carolina-ribeiro@edu.ulisboa.pt

Q_0^2 and Q^2 by:

$$\Delta\left(Q^2, Q_0^2\right) \simeq \exp\left\{-\int_{Q_0^2}^{Q^2} \frac{\mathrm{d}\mu^2}{\mu^2} \frac{\alpha(\mu^2) C_F}{\pi} \int_{z_{\min}}^{z_{\max}} \frac{\mathrm{d}z}{z}\right\}, \quad (1)$$

where μ corresponds to the phase space ordering variable, essentially representing the quantity controlling the emissions; α, which we considered ≈ 0.1179, is related to the coupling scale for this work [4, 7]; $C_F = 4/3$ being the quark colour factor and z the energy fraction of the emitted particle with respect to its emitter. With the coupling scale fixed, we now need to choose the ordering variable (in our case, it will be set to be the invariant mass, m) and its respective range.

Since the Sudakov form factors are based on perturbative QCD and we wish only to work in the parton shower regime and not focus in the hadronization, we also considered the minimum invariant mass to be of the order of the proton rest mass ($\approx$ 1 GeV). With that we can generate the energy fraction to then compute the ordering variable. The Sudakov form factor boundaries are explained in subsection 2.2 and the generation details are explained in subsection 2.3.

2.1 Initial Conditions and Assumptions

We considered a simple model, where a very energetic ($p_z \approx 10^3$GeV) quark emits a single gluon, using light-cone coordinates in momentum space. In this space, the usual Minkowski coordinates are given by: $p = (E, px, py, pz)$ in natural units. We can rotate the $px - py$ plane by 45°, obtaining the referred light-cone coordinates, given by $p = ((E + p_z)/\sqrt{2}, (E - p_z)/\sqrt{2}, p_x, p_y) = (p^+, p^-, p_x, p_y)$. It is important to note that in the ultra-relativistic limit, where the rest mass of the particle is negligible in comparison to its energy, we have $E \sim p_z$ and therefore p^- is also negligible.

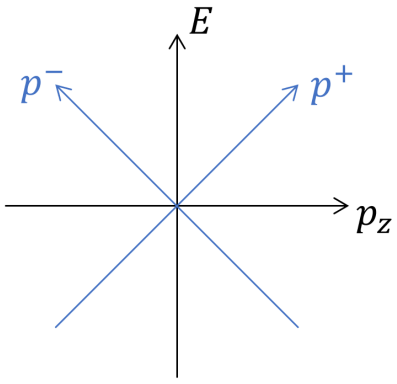

Figure 1: Transformation from Minkowski to Light-cone coordinates regarding the $E - p_z$ plane.

In Figure 1 we show a visualisation of the transformation from Minkowski to Light-cone coordinates. Working in these coordinates, we assume in the emission the conservation of the " + " momentum component and no deflection of the mother quark in the process, meaning the quarks travel in a straight line. For simplicity, we assume this direction to be the z-axis, this choice being nevertheless arbitrary. Furthermore, we assumed the gluons to have very low energy - this is justified by noticing that the probability for the gluon to carry a fraction z of the mother quark is given by $1/z$, as seen in eq.(1). This way the energy fraction $z = k_n^+/p_{n-1}^+$, with k_n^+ and p_{n-1}^+ being the gluon and mother quark "+" momentum component, respectively, is also small (soft limit). This condition assures the gluon invariant mass to be low enough so as to neglect the possibility of emissions from it, and in this model, the parton shower evolution reduces essentially to the simple quark-gluon emission. A visualisation of this process is depicted in Figure 2, where the relevant kinematic variables were made explicit.

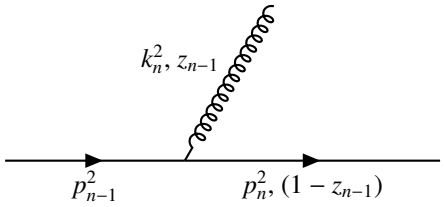

Figure 2: Feynman diagram representing our model. A quark with an initial light-cone momentum p_{n-1}^+ and an invariant mass of p_{n-1}^2 emits a single gluon with light-cone momentum of $k_n^+ = p_{n-1}^+ z_{n-1}$ and an invariant mass of k_n^2, without recoil.

2.2 Kinematic limits

As mentioned previously, we considered only the conservation of the "+" momentum component. The conservation of all the momentum components ("+", "−" and "⊥") would imply:

$$p_{n-1}^2 - \frac{k_n^2}{z_{n-1}} - \frac{p_n^2}{(1 - z_{n-1})} = \frac{\left|\boldsymbol{p}_{\perp n,\,\mathrm{rel}}\right|^2}{z_{n-1}\,(1 - z_{n-1})} \geq 0, \quad (2)$$

with $\boldsymbol{p}_{\perp n,\,\mathrm{rel}}$ being the relative transverse momentum between the emitted gluon and the daughter quark:

$$\boldsymbol{p}_{\perp n,\,\mathrm{rel}} = z_{n-1}\boldsymbol{p}_{\perp n} - (1 - z_{n-1})\boldsymbol{k}_{\perp n} \quad (3)$$

However, since we assumed that the emitted gluons cannot radiate further, their invariant mass is small, and we can therefore neglect its invariant mass term. Despite z being small, as we shall see, its minimum value is truncated, and this term will not diverge. Furthermore, since emissions are exponentially far from one another in the invariant mass scale, we can also neglect the invariant mass term of the daughter with respect to the mother. This way we simply have:

$$p_n^2 \approx \frac{|\boldsymbol{p}_{\perp n,rel}|^2}{(1 - z_n)z_n}. \quad (4)$$

We can impose a minimum value for the relative transverse momentum, related with the invariant mass threshold referred in the beginning of this section. By imposing a minimum value on the former, we are also implying a minimum resolution between the gluon and daughter quark, essentially assuring that both are sufficiently separated from one another so that we can distinguish them. This is a way of visualizing the hadronization stopping condition. By considering then a condition of the form $|\boldsymbol{p}_{\perp n,rel}|^2 \geq K^2_{\text{had}}$, we have for the energy fraction z:

$$\frac{K^2_{\text{had}}}{p^2_n} \leq (1 - z_n)z_n \leq \frac{1}{4} \tag{5}$$

By taking the upper bound of the square roots for simpler z limits we have our conditions for the limits on z:

$$z_{min} = 1 - z_{max} = \frac{K^2_{had}}{p^2_n} \tag{6}$$

It is important to refer that since we are using upper bounds for the kinematic limits some emissions will not be physically possible. The workaround will be to include a kinematic veto that will discard this emission and try to generate a new one until the lower limit is reached [8]. We detail this procedure in the end of subsection 2.3.

Finally, the boundary values for the invariant mass can be obtained using again the previous relation:

$$4K^2_{\text{had}} \leq p^2_n \leq p^2_{n-1}. \tag{7}$$

2.3 Sampling variables

To generate the emissions, we created a simple Monte Carlo by making use of the Sudakov form factors, referred in the beginning of this section, and the technique of *inverse sampling* [9].

In the latter we first compute the cumulative distribution, assign a random value to it and finally invert it. This method can be better understood by looking at figure 3 where a random cumulative distribution is shown.

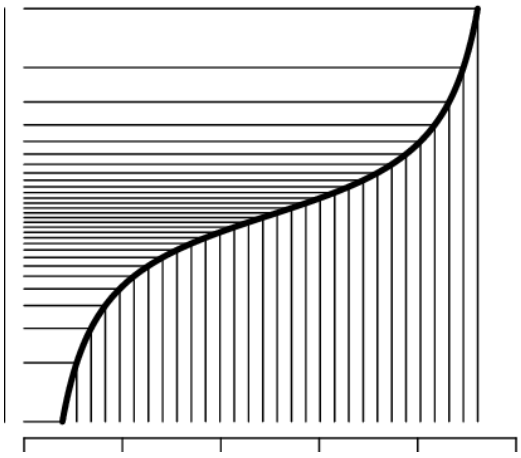

Figure 3: Cumulative distribution of a general function and comparison between the width of each horizontal bin and the width of its respective vertical bin. All horizontal bins have the same width. Figure taken from [9].

In the figure we can see the relation between the width of each horizontal bin and the width of its respective vertical bin. As we can observe, the regions were the slope of the cumulative distribution is lower correspond to smaller vertical bin width and vice-versa. This way if the vertical bin width is lower than the respective horizontal one, this value is less likely to be generated since the slope of the cumulative distribution corresponds to the actual probability distribution.

The cumulative distribution for the scale of an emission can be computed from the ratio of Sudakov factors:

$$\Delta\left(p^2_{n,max}, Q^2\right) = \frac{\Delta\left(p^2_{n,max}, 4Q^2_{had}\right)}{\Delta\left(Q^2, 4Q^2_{had}\right)}. \tag{8}$$

Solving the ratio by substituting in each case the respective scales for p^2_n, and using the z boundary values showed in the previous subsection, we obtain:

$$\begin{aligned}\Delta\left(p^2_{n,\max}, p^2_n\right) &= \frac{\Delta\left(p^2_{n,\max}, Q^2_{\min}\right)}{\Delta\left(p^2_n, Q^2_{\min}\right)} \\ &\simeq \exp\left\{-\frac{\alpha C_F}{2\pi}\left(\ln^2\frac{p^2_{n,\max}}{Q^2_{\text{had}}} - \ln^2\frac{p^2_n}{Q^2_{\text{had}}}\right)\right\}.\end{aligned} \tag{9}$$

We can now make use of the inverse sampling technique, obtaining:

$$\begin{aligned}&\Delta\left(p^2_{n,\max}, p^2_n\right) = \mathcal{R}_\Delta \Leftrightarrow \\ &p^2_n = Q^2_{\text{had}}\,\exp\left\{+\sqrt{\ln^2\frac{p^2_{n,\max}}{Q^2_{\text{had}}} + \frac{2\pi}{\alpha C_F}\ln\mathcal{R}_\Delta}\right\}\end{aligned} \tag{10}$$

Now for the energy splitting, z, we have:

$$F(z_n) \overset{\text{def}}{=} \frac{\int_{z_{\min}}^{z_n} \mathrm{d}u/u}{\int_{z_{\min}}^{1-z_{\min}} \mathrm{d}u/u} = \frac{\ln\left(z_n/z_{\min}\right)}{\ln\left(1/z_{\min} - 1\right)} \tag{11}$$

Inverting again we obtain:

$$R_z = F(z_n) \Rightarrow z_n = \frac{Q^2_{had}}{p^2_n}\left(\frac{p^2_n}{Q^2_{had}} - 1\right)^{R_z} \tag{12}$$

The process for accepting the generated z and p^2_n goes as follows. First we generate p^2_n assuming $p_{n,max} = p^2_{n-1}$ and check whether condition (7) is verified. If it is not, then the shower ends; otherwise, we proceed to generate a z value. If then the condition (5) is not verified we regenerate p_n, assuming the new maximum value to be the previously generated one, $p_{n,max} = p_{n,gen}$ (veto procedure). This process is repeated until both conditions are verified or we reach the stopping condition.

2.4 Extracting the Kinematics

By following the presented method we can simulate parton showers for the considered model, and then compute the kinematics of the process in order to understand how

the shower evolution is dependent on certain variables. It is important to highlight that the shower generation and further kinematic extraction is done in the center of mass (CM) frame of the mother quark, in which $\vec{p_\perp} = \vec{0}$. The results presented in Section 3 are nevertheless consistent with the laboratory frame. We applied the respective boost factor after computing the relevant kinematics.

Our algorithm receives the initial momentum in the z-axis as input. Unless stated otherwise, this value was fixed to $p_z = 1$ TeV. We can then compute the initial quark energy by the Einstein relation, and with that compute the initial 4-momentum in light-cone coordinates. After this first iteration, we simply use the z definition to compute the "+" momentum component of the quark and gluon and the "−" momentum component of the quark by using the 4-momentum norm. These relations are summarised below:

$$p_n^+ = p_{n-1}^+(1 - z_{n-1}) \tag{13}$$

$$p_n^- = \frac{p_n^2}{2p_n^+} \tag{14}$$

$$k_n^+ = p_{n-1}^+ z_{n-1}, \tag{15}$$

where for simplicity we assumed the "⊥" components to be zero.

We also computed the transverse momentum of the gluon and the angle θ with respect to its mother. Going back to equation (3) we neglect the quark term since we are working in the soft limit ($z \ll 1$):

$$|\boldsymbol{p}_{\perp n,\,\mathrm{rel}}| \approx (1 - z_{n-1})|\boldsymbol{k}_{\perp n}| \Rightarrow |\boldsymbol{k}_{\perp n}| = \sqrt{\frac{z_{n-1}p_{n-1}^2}{1 - z_{n-1}}}. \tag{16}$$

Finally, the opening angle θ can also be computed by:

$$|\boldsymbol{k}_{\perp n}| = |\boldsymbol{k}_n| \sin\theta_n = E_{n-1} z_{n-1} \sin\theta_n \tag{17}$$

$$\Rightarrow \theta_n = \arcsin \frac{|\boldsymbol{k}_{\perp n}|}{z_{n-1} E_{n-1}} = \tag{18}$$

$$= \arcsin \frac{\sqrt{2}|\boldsymbol{k}_{\perp n}|}{z_{n-1}\left(p_{n-1}^+ + p_{n-1}^-\right)} \tag{19}$$

3 Results

3.1 Evolution over emissions

Taking the procedure listed in section 2.4, we generated 100 000 showers. First, we studied the overall evolution of the shower, computing the relevant kinematics over the first emissions.

In Figure 4 we show the z (top panel) and θ (bottom panel) distributions over the first three emissions in orange, purple and green, respectively. As we can see, the z distribution increases as we go further in emissions. This can be explained by looking at equation (5); z increases as p_n decreases, and as the quark emits gluons, its invariant mass decreases.

Now looking at the θ distribution, there is an overall decrease from the first to the third emission. This phenomena is essential regarding the jets' collimation: if the shower did not get more collimated as it developed, then it would not be possible to detect jet-like structures in the event. The collimated structure is due to (i) the decreasing angle in subsequent emissions and (ii) the boost of the particles. Without this, it would be much harder to try to reconstruct the collision event.

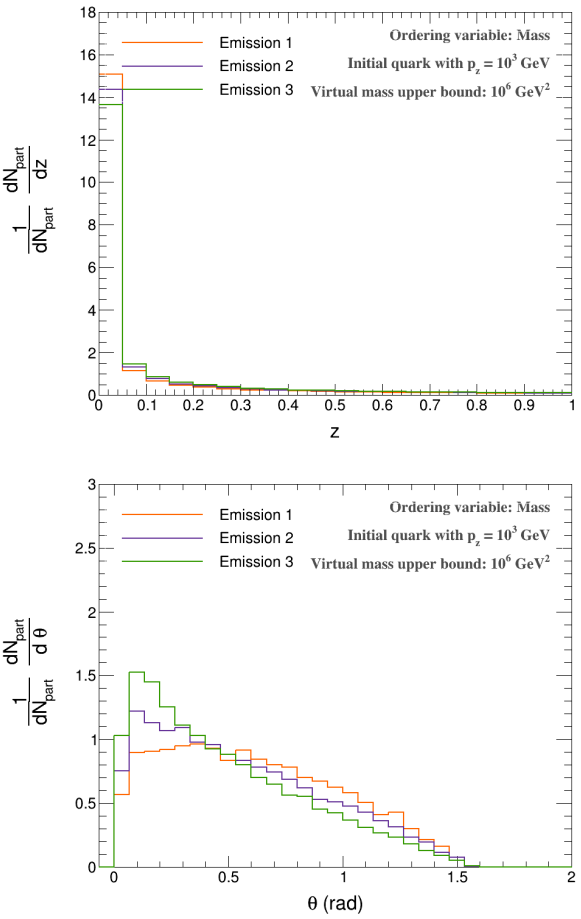

Figure 4: z (top panel) and θ (bottom panel) normalized distributions for the first three emissions.

After this, we computed the Lund planes [10, 11], a bi-dimensional representation of the (z, θ) space per emission. These planes essentially comprise the relevant splitting information, making the overall visualization of the evolution more simple. As shown further we can even assign a value for each emission, enabling us to actually see the "trajectory" described by the parton shower.

The Lund planes for the first three emissions can be seen in Figures 5, 6 and 7. The axis are represented in logaritmic scale as $(\log_{10}(\pi/\theta), \log_{10}(1/z))$. As such, higher values in the (x, y) direction represent instead lower absolute values of (θ, z). The density along the z direction, represented by the colour scheme, helps to understand where the majority of the emissions are located in this bi-dimensional plane. The evolution along z is not so visible, but in θ, there is a clear displacement towards the right (smaller θ) direction. The visualization of each emission alone is not as useful for our purposes since we want in-

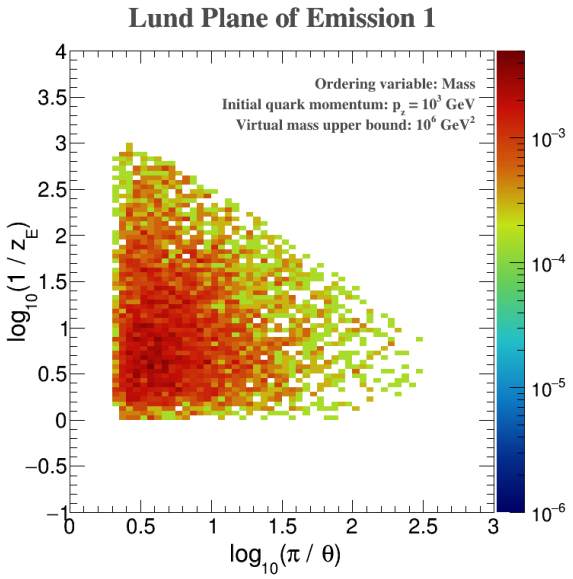

Figure 5: Lund planes with z vs θ values for the first emission.

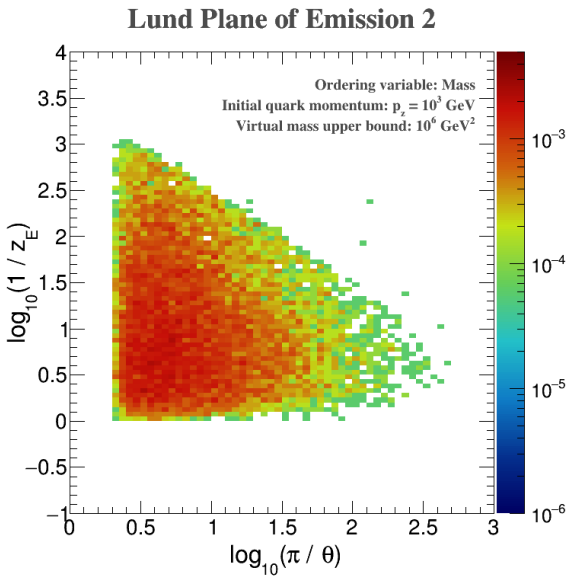

Figure 6: Lund planes with z vs θ values for the second emission.

stead to understand how the full parton shower evolves. As such, to make this visualisation clearer, we computed the average of these Lund plane for the first six emissions. Each Lund plane is then represented as single point. The full sequence can now be represented in a single Lund plane shown in Figure 8 (green dots).

Looking at this plot we can clearly trace down the evolution from the first to the sixth emission. Starting from the upper left corner of this plane (small z and high θ), subsequent emissions will follow an increase in the value of z and a decrease in θ.

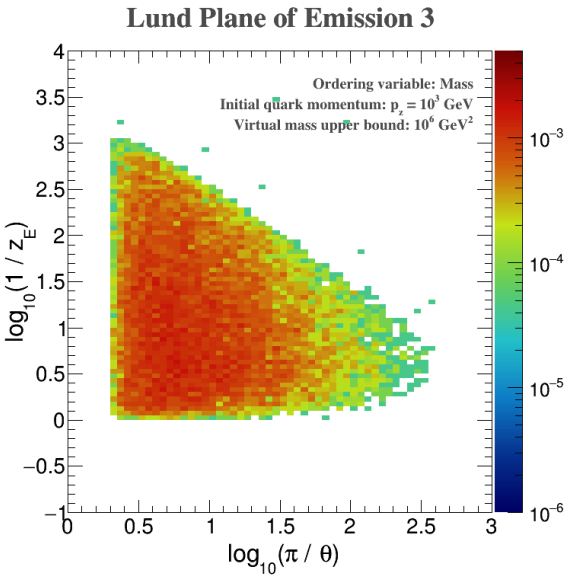

Figure 7: Lund planes with z vs θ values for the third emission.

3.2 Varying initial momentum

We then studied the differences in the parton shower evolution when considering a different value for the initial momentum.

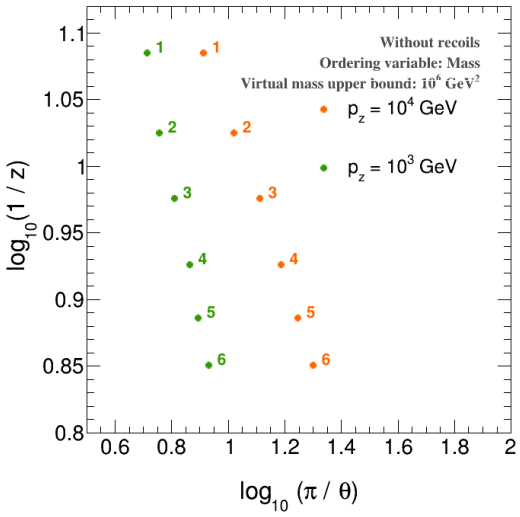

Figure 8: Comparison between the first six emissions for an initial momentum of 10^4GeV and 10^3GeV. Each point represents the average of the respective Lund plane for that emission.

In Figure 8 we show directly the results of the Lund plane averages for the first six emissions considering our initial momentum of 10^3 (green dots) and comparing to an initial quark of 10^4 GeV (orange dots). The z distribution seems the same, which we would expect looking at equa-

tion (12). This shows that, for the considered model, the random generation in the Toy Monte Carlo model is independent of the initial momentum. However, there is an overall decrease in θ with the increase of the initial momentum. This shift can be explained by the boost factor explained above. Since the initial quark has a larger momentum, the boost will be higher and the shower will be more collimated.

3.3 Relaxing Kinematic Restrictions

Finally, we compared the obtained results for this model with one that enables the quark to deflect slightly when it emits a gluon [6]. The respective Feynman Diagram is shown in Figure 9 (our prescription in which the quark does not recoil is illustrated in Figure 2).

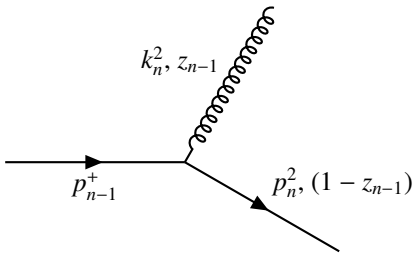

Figure 9: Feynman diagram representing the recoil model. A quark with an initial light-cone momentum p_{n-1}^+ and an invariant mass of p_{n-1}^2 emits a single gluon with light-cone momentum of $k_n^+ = p_{n-1}^+ z_{n-1}$ and an invariant mass of k_n^2, being then deflected.

The resulting averages of the Lund plane, for the first six emissions, and for an initial quark with $p_z = 10$ TeV are illustrated in Figure 10. Our model without recoils is illustrated in orange dots and the model with recoils in purple dots. It is important to remember that θ is measured with respect to the mother quark direction for both models, otherwise, no comparison could be made.

Both methods start with the same initial conditions, as expected. Regarding the evolution, the recoil model develops overall in the same way but more steep and pronounced than the one with no recoil. The greater decrease in θ is related with the increase in the quark "freedom". In the recoil model some of the deflection can be distributed to the quark and the gluon can therefore have smaller angles with respect to the mother propagation axis.The greater increase in z is explained by the difference in kinematic restrictions in the recoil model. In this model, 4-momentum conservation was assumed, so certain pairs of (z, p_n^2) values are not allowed, resulting in the referred jumps in the Lund plane.

4 Conclusions

In this project we developed a simple parton shower model in which a quark is allowed to emit low-energy gluons without being deflected in the process.

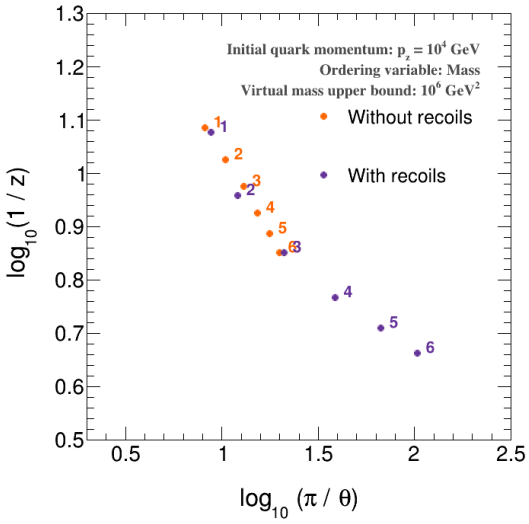

Figure 10: Comparison between the first six emissions for the recoil and no recoil models. Each point represents the average of the respective Lund plane for that emission.

We found, as we go further in each emission, an increase in the value of energy fraction carried by the gluon (z) and a decrease in the value of its emission angle (θ). This angular behaviour plays an important role regarding the formation of jet collimated-like structures. As the angle decreases the shower gets more collimated, making it easier to then detect it experimentally.

When increasing the initial quark momentum the value for z stayed the same, while θ decreased, due to a boost factor.

Finally, we compared our parton shower results with another model where the quark is allowed to recoil in each gluon emission. We observed that, despite the kinematic refinements, z and θ maintained their overall evolution. We noticed however that evolution to be more pronounced for the recoil model.

Acknowledgements

Special thanks to André Cordeiro and professor Liliana Apolinário for making this internship possible and sparking the curiosity for this area. Our gratitude for all guidance but also to all the patience and dedication in covering and expanding all our doubts.

References

[1] G.P. Salam, CERN Yellow Rep. School Proc. **5**, 1 (2020)

[2] R.K. Ellis, W.J. Stirling, B.R. Webber, *QCD and collider physics*, Vol. 8 (Cambridge University Press, 2011), ISBN 978-0-511-82328-2, 978-0-521-54589-1

[3] G.P. Salam, Eur. Phys. J. C **67**, 637 (2010), 0906.1833

[4] R.L. Workman, Others (Particle Data Group), PTEP **2022**, 083C01 (2022)

[5] L. Apolinário, Y.J. Lee, M. Winn (2022), 2203.16352

[6] A. Cordeiro, Master of Science Degree Thesis **Engineering Physics**, IST, Lisbon University (2021)

[7] L. Susskind, Phys. Rev. **165**, 1535 (1968)

[8] B.R. Webber, Annual Review of Nuclear and Particle Science **36**, 253 (1986), https://doi.org/10.1146/annurev.ns.36.120186.001345

[9] S. Holmes, S. Rubinstein-Salzedo, C. Seiler (2015)

[10] A.J. Larkoski (2017), 1709.06195

[11] H.A. Andrews et al., J. Phys. G **47**, 065102 (2020), 1808.03689